The Journal of Experimental Biology **198**, 2619–2629 (1995)
Printed in Great Britain © The Company of Biologists Limited 1995
JEB0053

IMMUNOLOCALIZATION OF PROTON PUMPS (H^+-ATPase) IN PAVEMENT CELLS OF RAINBOW TROUT GILL

GARY V. SULLIVAN[1], JAMES N. FRYER[2] AND STEVE F. PERRY[1,*]

[1]*Department of Biology, University of Ottawa, 30 Marie Curie, Ottawa, Ontario, Canada K1N 6N5* and [2]*Department of Anatomy and Neurobiology, University of Ottawa, 452 Smyth Road, Ottawa, Ontario, Canada K1H 8M5*

Accepted 15 August 1995

Summary

The expression of the V-type proton ATPase (H^+-ATPase) was examined in the gill of the freshwater rainbow trout (*Oncorhynchus mykiss*) using immunocytochemistry in concert with laser scanning confocal or electron microscopy. A synthetic peptide consisting of the carboxy-terminal region of the 31 kDa subunit of the bovine renal H^+-ATPase was used to generate an antiserum in rabbits, and its suitability for use in trout gill was confirmed by western blotting.

Gill epithelial cells demonstrated specific immunoreactivity, the intensity of which was increased markedly after 18 h of exposure to hypercapnia (1 % CO_2 in air). The increased intensity of H^+-ATPase immunoreactivity was associated with elevated branchial net acid excretion. In the hypercapnic fish, the specific immunoreactivity was associated with both the apical membrane and cytoplasm. Electron microscopy revealed that specific immunoreactivity was localized to the pavement cells and was particularly associated with the apical membrane and subapical cytoplasmic vesicles.

The increased H^+-ATPase immunoreactivity in the epithelial cells of hypercapnic fish and the increased intensity of the immunoreactive bands in western blots from hypercapnic fish demonstrate an 'up-regulation' of this protein in response to respiratory acidosis. The results are discussed with reference to current models of acid–base and ion regulation in the gill of freshwater fish.

Key words: *Oncorhynchus mykiss*, rainbow trout, H^+-ATPase, pavement cell, laser scanning confocal microscopy, gill epithelium, immunocytochemistry.

Introduction

In freshwater teleosts, Na^+ and Cl^- are absorbed across the gill epithelium from the dilute external environment. This serves to counterbalance the continual loss of these ions by diffusion or by renal excretion and thereby to establish ionic balance (see review by Evans, 1993). There is a general consensus, arising from the results of numerous indirect studies, that Cl^- uptake is achieved by a Cl^-/HCO_3^- exchange mechanism located on the apical membranes of branchial chloride cells (for reviews, see Goss *et al.* 1992*a*; Avella and Bornancin, 1990; Perry and Laurent, 1993; Shuttleworth, 1989; McDonald *et al.* 1989). The nature of Na^+ uptake, however, is less certain and currently there is considerable debate surrounding its mechanism and cellular location. In recent years, the classical model incorporating an electroneutral Na^+/H^+ exchanger (Krogh, 1938) has been challenged on the basis of (i) thermodynamic criteria (Avella and Bornancin, 1989), (ii) analogy with other acid-excreting 'tight' epithelia (Goss *et al.* 1995), and (iii) the results of several studies using an array of pharmacological (Lin and Randall, 1991), biochemical (Lin and Randall, 1993) and morphological (Lin *et al.* 1994; Laurent *et al.* 1994) techniques. The new model of Na^+ uptake across the gill epithelium of freshwater fish incorporates an electrogenic apical membrane proton pump that establishes a favourable electrochemical gradient for the inward movement of Na^+ through apical membrane Na^+ channels. The most compelling evidence for this model emanates from the recent work of Lin *et al.* (1994), in which proton pump (vacuolar-type H^+-ATPase) immunoreactivity was clearly demonstrated in the gill of rainbow trout. However, the branchial cell type in which the proton pump/Na^+ channel is localized is less obvious and is currently debated. Lin and Randall (1991) proposed that the mitochondria-rich chloride cell was the site of the proton pump/Na^+ channel mechanism, yet recent immunocytochemical results (Lin *et al.* 1994) suggest that proton pumps are distributed in both chloride cells and pavement cells. The low resolution of the light microscopy

*Author for correspondence.

techniques employed by Lin *et al.* (1994), however, did not permit precise identification of the immunoreactive cells. Laurent *et al.* (1994), employing transmission electron microscopy, identified presumptive proton pump vesicles that were located almost exclusively in pavement cells. Furthermore, Morgan *et al.* (1994) concluded, on the basis of X-ray microanalysis, that the pavement cell is the site of the Na^+ uptake mechanism in brown trout (*Salmo trutta*). These results concur with the findings of Goss *et al.* (1992*b*), who observed physical covering of gill chloride cells by pavement cells in hypercapnic brown bullhead (*Ictalurus nebulosus*) at times of stimulated acid excretion and Na^+ uptake. Owing to the absence of any correlation between Na^+ uptake and chloride cell surface area in hypercapnic fish, Goss *et al.* (1992*b*) postulated that the pavement cell was involved in Na^+ absorption and H^+ excretion.

With this general background, the primary goals of the present study were (i) to provide direct evidence for the localization of the proton pump in the pavement cell of the rainbow trout gill and (ii) to establish its role in acid–base balance. These goals were accomplished by evaluating the gills of normocapnic and hypercapnic fish using immunological techniques in conjunction with laser scanning confocal and electron microscopy.

Materials and methods

Experimental animals

Rainbow trout [*Oncorhynchus mykiss* (Walbaum)] weighing 245–310 g were obtained from Linwood Acres trout farm (Cambellcroft, Ontario, Canada) and held in large (300 l) fibreglass tanks supplied with flowing, dechlorinated City of Ottawa tapwater (P_{O_2}=20.0–21.3 kPa, P_{CO_2}=0.033–0.047 kPa, $[Na^+]$=0.15 mmol l^{-1}, $[Cl^-]$=0.18 mmol l^{-1}, $[Ca^{2+}]$= 0.42 mmol l^{-1}, temperature 10 °C). All fish were maintained in the aquarium for a minimum of 4 weeks prior to experimentation and were fed to satiation on alternate days with a commercial salmonid diet. They were not fed for 24 h prior to experimentation. The photoperiod was held at 12 h:12 h L:D.

Surgical procedures

Fish were anaesthetized in a 1:10 000 (w/v) solution of MS 222 (Sigma) buffered to pH 7.0 with $NaHCO_3$. To allow blood sampling, indwelling dorsal aortic (DA) cannulae were surgically implanted according to the procedure of Soivio *et al.* (1975). Fish were placed into individual, opaque acrylic boxes (approximate volume 3 l) and allowed to recover for at least 24 h prior to experimentation.

Hypercapnia

Five periods were examined in the present study: control (pre-hypercapnia) and after 12, 18, 24, 36 and 48 h of hypercapnia (1 % CO_2 in air; $P_{W}CO_2$=1.01 kPa). In order to induce respiratory acidosis, the inflowing water was rendered hypercapnic by bubbling a mixture of CO_2 in air (Wösthoff gas-mixing pump) through a gas equilibration column (Perry *et al.* 1987*a*,*b*) to obtain a final $P_{W}CO_2$ of 1.01 kPa. $P_{W}CO_2$ was monitored continuously by circulating inflowing water through a P_{CO_2} electrode (E5037; Radiometer) connected to a meter (PHM 72; Radiometer) and chart recorder. The final 3 h of each exposure period was used as a flux period during which water flow was stopped and hypercapnia was maintained by bubbling 1 % CO_2 in air (commercial gas cylinders) directly into individual boxes.

Acid–base parameters

Upon concluding each of the flux periods, a 1 ml blood sample was taken from the DA cannula of each fish for immediate analysis of acid–base variables. A 10 ml water sample was also taken from each box at the beginning and end of each flux period for measurements of titratable alkalinity (TA) and total ammonia concentration ($[NH_3]$). Whole-blood pH was determined with a microcapillary electrode (Radiometer G299A) in conjunction with a Radiometer PHM 71 acid–base analyzer and a BMS3 Mk2 Blood Microsystem thermostatted to 10 °C. Blood was centrifuged (12 000 ***g***) for 30 s and plasma total CO_2 was measured on 50 μl samples using a total CO_2 analyzer (Corning model 965). Plasma bicarbonate (HCO_3^-) concentrations were calculated from the total CO_2 and pH measurements according to the Henderson–Hasselbalch equation and appropriate constants (Boutilier *et al.* 1984). Water $[NH_3]$ was determined colorimetrically by the salicylate–hypochlorite method (Verdouw *et al.* 1978) and TA and net acid fluxes were determined as described by McDonald and Wood (1981).

Tissue preparation

At the end of each experimental period, the second and third gill arches from the right and left gills were removed from control and hypercapnic fish and immediately emersion-fixed for immunocytochemistry (ICC) using procedures appropriate for either light or electron microscopy. The gills of 12–16 fish were examined for each period of hypercapnia or normocapnia. Upon close examination, it was determined that gills from the 18 h hypercapnic fish exhibited the most intense immunoreactive signal; therefore, four additional groups (36 fish) were exposed to 18 h of hypercapnia. For light microscopy, the tissue was rinsed briefly in cold phosphate-buffered saline (PBS) and then placed in Bouin's fixative for 2 h, followed by three 10 min washes in cold PBS and finally 24 h of fixation in Bouin's fixative without acetic acid. For electron microscopy, the tissue was rinsed briefly in cold PBS and immersed for 24 h in a fixative designed for immunoelectron microscopy (4 % paraformaldehyde, 0.1 % glutaraldehyde, 0.1 % picric acid in PBS). All tissues were then dehydrated in a series of ethanols (12 h in 70 % ethanol, 2 h in 90 % ethanol, 2 h in 95 % ethanol, two times 2 h in 99 % ethanol). Tissue for light microscopy was trimmed to remove any bone, and a portion of gill arch with 7–12 lamellae was obtained. These were placed in xylene (twice for 1 h each time) and then in paraffin (Ameraffin, Baxter Diagnostics Inc.) at

60 °C for 12 h, to allow infiltration, before embedding in paraffin blocks. For immunoelectron microscopy, individual lamellae were removed from gill arches and trimmed to a length of approximately 2 mm. This tissue was placed in a solution of 50 % ethanol/50 % LR White acrylic resin (J.B. EM Services Inc.) for 2 h and then transferred to LR White resin for 2 h. Finally, the pieces of tissue were embedded in LR White resin (a water-soluble embedding medium) in gelatin capsules (no. 00, T.U.B. Enterprises) and allowed to cure overnight at 60 °C.

Immunological techniques

An antiserum was raised in rabbits against the carboxy-terminal peptide of the 31 kDa subunit of the bovine renal V-type ATPase (Cys-Gly-Ala-Asn-Ala-Asn-Arg-Lys-Phe-Leu-Asp; Hirsch *et al.* 1988). Pre-immune blood samples were drawn from two rabbits and the serum was collected, frozen and stored at −80 °C. Rabbits were inoculated with the peptide antigen and blood samples were drawn after 6 weeks. Serum was frozen and stored at −80 °C. Rabbits were then boosted with another inoculation and a second bleed was performed after 6 weeks. When tested on rat kidney, the serum obtained from the second bleed resulted in the strongest immunoreactive signal (Y. Okawara, personal communication). Sections (7 μm) were cut from paraffin blocks using a microtome, mounted on glass slides, and allowed to dry on a slide warmer for at least 6 h. Sections were incubated overnight at room temperature with primary antiserum diluted 1:500 in Tris buffer (0.1 mol l^{-1} Tris and 0.14 mol l^{-1} NaCl) containing 0.6 % carrageenan and 0.3 % Triton X-100 (TCT). After washes in Tris buffer (twice for 7 min each time), sections were incubated with biotinylated anti-rabbit secondary antibody diluted 1:50 with TCT for 30 min. Following another series of washes, final labelling was performed with a 30 min incubation in Streptavadin-CY3 (Sigma) diluted 1:50 in TCT. Positive immunoreactivity was visualized using fluorescence microscopy and confocal microscopy. Confocal images were generated by an upright confocal laser scanning microscope (Leica) using an air-cooled krypton/argon laser. Specific immunoreactivity (Steptavidin-CY3 conjugate, Sigma) was visualized following excitation at a green wavelength (545±20 nm). In order to visualize the entire gill tissue, images were generated from excitation at a red wavelength (580±34 nm) which caused autofluorescence of the tissue. To ensure valid comparisons between fish and treatment groups, all settings for the confocal microscope and laser were kept constant.

Thin sections (50–60 nm) for immunoelectron microscopy were cut using an ultramicrotome and collected on nickel grids. Sections were incubated overnight in antiserum diluted 1:500 in TBS–Tween (Tris-buffered saline and Tween). Sections were then washed in TBS (3×5 min) and incubated with biotinylated anti-rabbit secondary antibody as above. Following another series of TBS washes, sections were incubated for 30 min in either Streptavadin–5 nm or –20 nm colloidal gold conjugate (Sigma). Sections were then briefly incubated with uranyl acetate (15 min) and lead citrate (7 min) in order to stain cellular structures. Visualization was achieved using transmission electron microscopy. Control sections for immunocytochemistry using light or electron microscopy were processed using secondary antibody only (primary antiserum was replaced with buffer), pre-immune serum in place of antiserum or primary antiserum which had been pre-incubated overnight with antigen (50 times excess antigen).

Western blotting

Fish were killed by a blow to the head. A cannula was inserted into the bulbus arteriosus and the gills were perfused *in situ* for approximately 3 min with ice-cold PBS. After the gills had been cleared of blood, the epithelial tissue was scraped from gill arches with a single-edged razor blade and collected in 0.75–1.0 ml of lysis buffer (Laemmli, 1970) containing protease inhibitors. Samples were boiled in 1.5 ml microcentrifuge tubes for 5 min and the tissue was homogenized with a 23 gauge needle and 1 ml syringe. Samples were centrifuged for 10 min at 9000 ***g***, and the

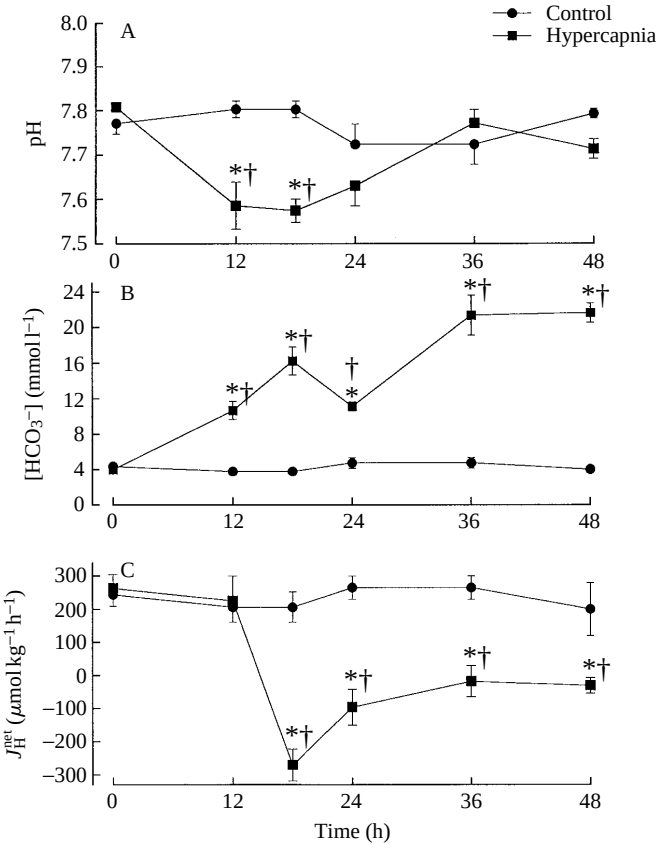

Fig. 1. The temporal effects of hypercapnia on blood pH (A), plasma bicarbonate concentration ($[HCO_3^-]$) (B) and branchial net acid excretion (J_H^{net}) (C) in control (filled circles) and hypercapnic (filled squares) fish. In C, positive values indicate acid equivalent uptake (base excretion) and negative values indicate acid equivalent excretion. * indicates a significant difference from control values. † indicates a significant difference from pre-hypercapnic values within the same group. Values shown are means ±1 S.E.M., N=6–8.

supernatant was collected and stored in 100 μl samples at −80 °C. Total protein in the samples was determined by the bicinchonic acid (BCA) method (Pierce). Electrophoresis was carried out on a vertical mini-gel apparatus (Bio-Rad) according to the procedure of Laemmli (1970) with a 12 % running gel. Tissue homogenates were diluted 1:1 with sample buffer and boiled for 5 min. Appropriate volumes of sample were loaded into each well to yield protein concentrations of 25 μg per well. Gels were run for 90 min at constant voltage (90 V) and equilibrated in transfer buffer for 30 min. Proteins were transferred to nitrocellulose using a mini Trans-Blot Cell (Bio-Rad) at a constant voltage (100 V) for 1 h. Membranes were blocked overnight with PBS containing 5 % skimmed milk. Membranes were washed three times in PBS and incubated for 90 min with a 1:2000 dilution of primary H^+-ATPase antiserum at room temperature. Membranes were then washed three times in PBS and incubated for 1 h in a 1:2000 dilution of biotinylated sheep anti-rabbit IgG (Sigma) at 10 °C. Membranes were again washed three times in PBS and then incubated for 1 h in a 1:5000 dilution of streptavadin–horseradish peroxidase conjugate. Finally, membranes were washed three times in PBS and immunoreactive bands were visualized using the ECL western blotting protocol on Hyperfilm-ECL (Amersham).

Image processing

All colour images were exported from the confocal microscope as TIFF (Tagged Image File Format) files and imported into a commercial software package (Adobe Photoshop). Western blots were scanned and imported as TIFF files into Adobe Photoshop. All images were treated in an identical manner, using minimal processing to enhance overall brightness and contrast. Finished images were pasted into Powerpoint (Microsoft) for final cropping, arrangement and labelling before printing.

Statistical analyses

Data shown in Fig. 1 are means ±1 standard error of the mean. Differences between the control and experimental fish were established using a two-tailed Student's *t*-test; the limit of significance was set at 5 %. Differences between experimental and pre-experimental values were established using a one-way analysis of variance (ANOVA).

Results

Acid–base parameters

Exposure to hypercapnia caused a significant, but transitory, reduction in arterial blood pH (Fig. 1A). Blood pH was

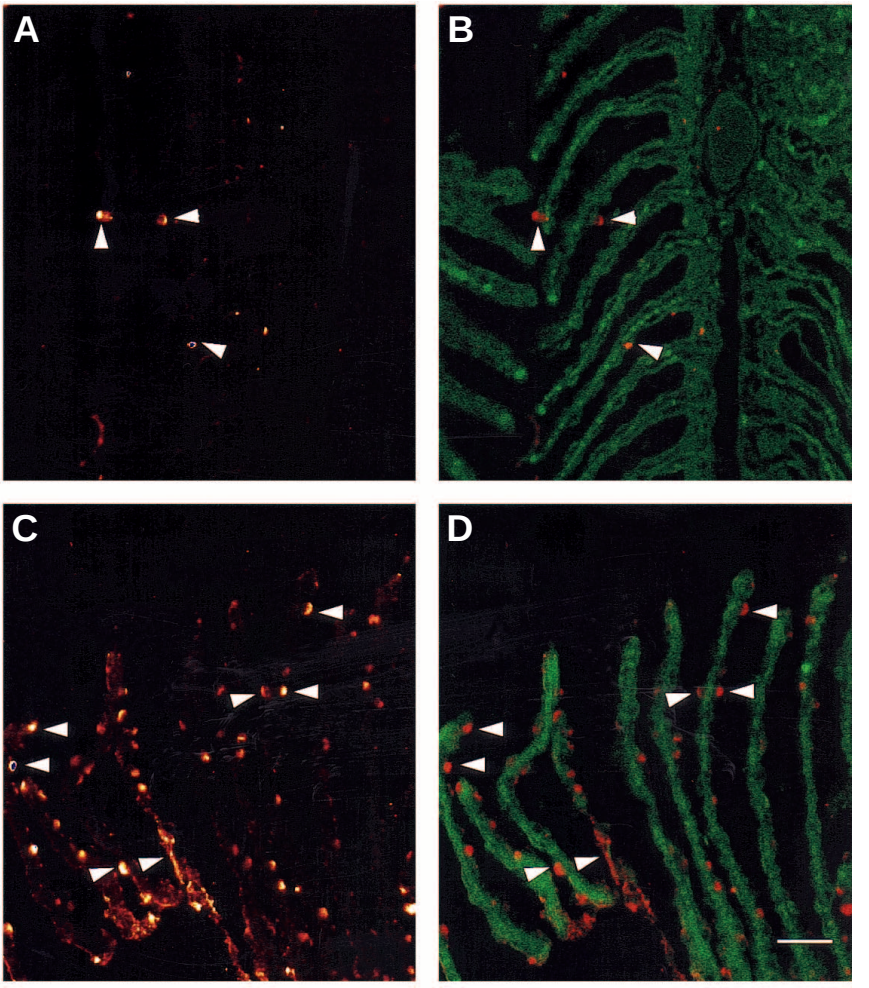

Fig. 2. Confocal micrographs of gills from normocapnic (A,B) and 18 h hypercapnic (C,D) trout showing specific immunoreactivity for the V-ATPase antibody (arrowheads). Note the increase in positive immunoreactivity both in intensity and in lamellar distribution in the gills of the hypercapnic fish. The images in A and C were generated by scanning with an excitation wavelength of 545±20 nm. Those in B and D make use of the autofluorescence properties of the tissue at an excitation wavelength of 580±34 nm (shown as green). The immunoreactive signal in B and D (arrowheads) is created by superimposing the first images onto this one. Scale bar, 50 μm.

reduced by approximately 0.2 units after 12–18 h but had returned to control values within 24 h. Plasma bicarbonate concentration displayed an immediate and sustained increase during the initial 36 h of hypercapnia and then stabilized at an elevated level (Fig. 1B). There was a pronounced increase in net H^+ excretion after 18 h of hypercapnia, as shown in Fig. 1C; net H^+ excretion remained at an elevated level throughout the 48 h period of hypercapnia. The control fish displayed no changes in any measured variable (Fig. 1).

Immunocytochemistry

Positive immunoreactive labelling for H^+-ATPase was clearly evident in the gills of both normocapnic or hypercapnic fish, and in both situations the labelling was localized to cells of the lamellar epithelium (Fig. 2). The intensity of labelling and the number of H^+-ATPase-immunoreactive cells was markedly increased during hypercapnia (e.g. compare Fig. 2A and Fig. 2C). Maximal labelling was achieved after 18 h of hypercapnia and this corresponded to the period of maximal net branchial H^+ excretion. Thus, while gill tissues from all time periods were examined, this study focuses on comparisons between 18 h of normocapnia and 18 h of hypercapnia.

Fig. 3 illustrates at higher magnification the pattern of proton pump immunolabelling in hypercapnic fish. While specific labelling was apparent on the majority of lamellar epithelial cells, a subpopulation of these cells displayed intense H^+-ATPase immunoreactivity. Specific labelling was abolished by incubating the gills of hypercapnic fish with pre-immune serum rather than antiserum (Fig. 3C,D) or by incubating with secondary antibody alone (Fig. 3E,F).

Figs 4 and 5 demonstrate that the H^+-ATPase immunoreactivity was localized to apical (water-facing) regions of lamellar epithelial cells. The intense thin band of immunolabelling apparent in Fig. 4B is reminiscent of the appearance of the pavement cell apical membrane and cytoplasm with respect to the flat, elongated morphology often observed in these cells. Serial optical sections through a single immunoreactive lamellar epithelial cell are shown in Fig. 5. These micrographs provide a partial three-dimensional

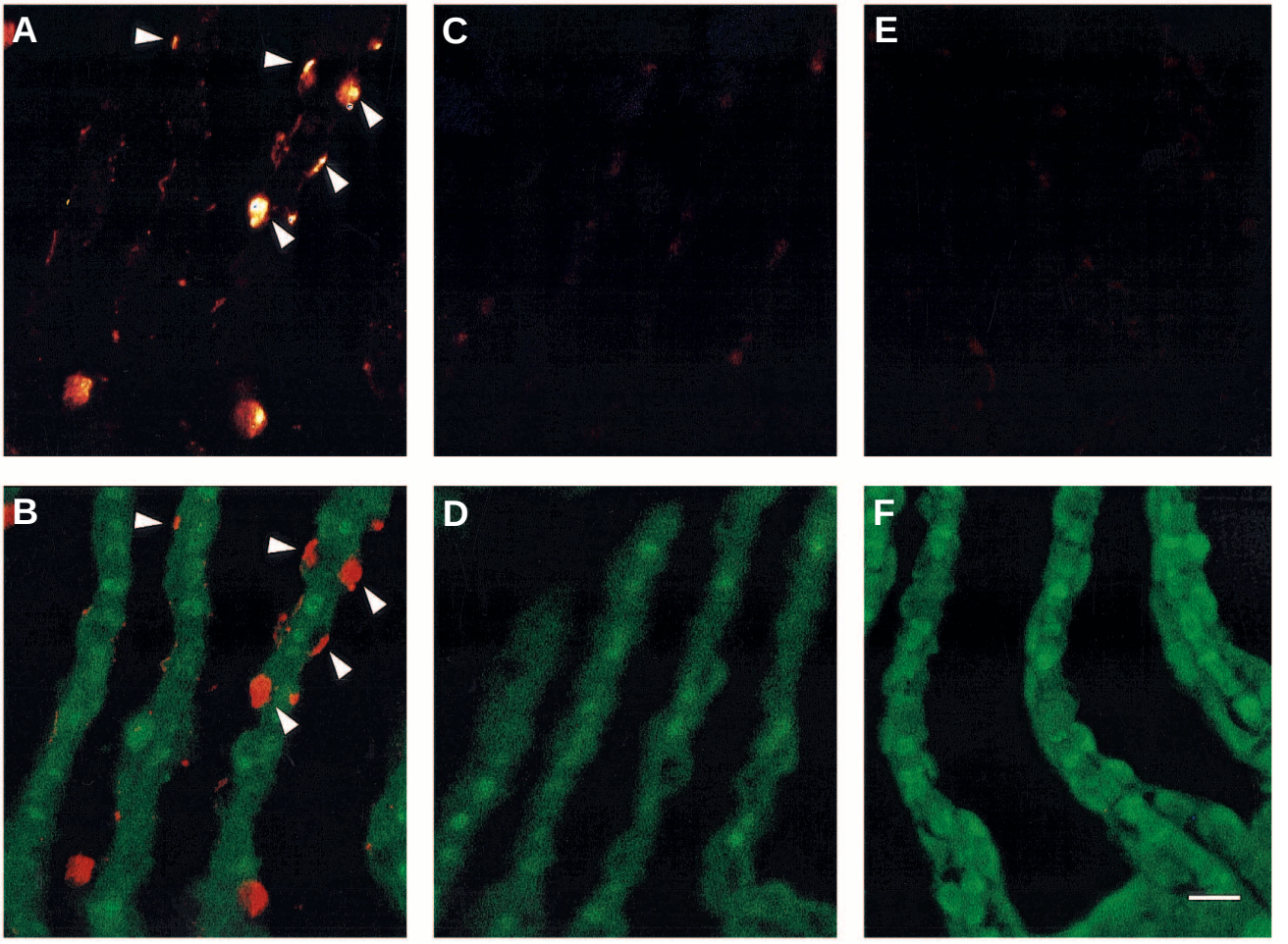

Fig. 3. Confocal micrographs of gills from hypercapnic fish. A and B show a gill section incubated with antiserum; immunopositive cells can be seen distributed over the lamellar surface (arrowheads). C and D show a gill section treated with pre-immune serum in place of antiserum. Specific immunoreactivity has been abolished. E and F show a gill section in which primary antiserum was replaced with buffer and incubation was with secondary antibody only. Again, no positive immunoreactivity is detectable. Images were obtained as described in Fig. 2. Scale bar, 15μm.

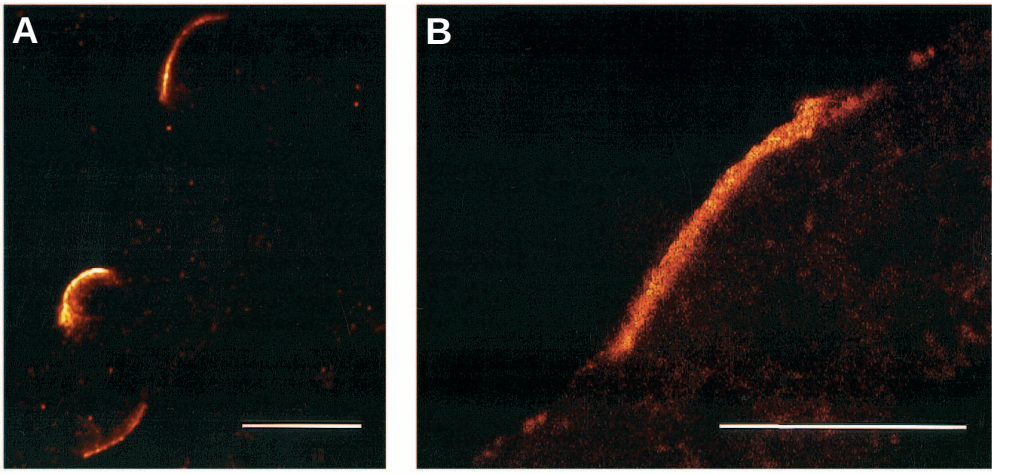

Fig. 4. (A,B) High-magnification confocal micrographs showing positive immunoreactivity associated with epithelial cells. The positive signal is apparently localized to the apical regions of the cells. Scale bars, 15 μm.

representation of the distribution of H^+-ATPase labelling within a cell. An optical section from the edge of the cell shows consistent labelling throughout the cell, this view representing a cut through, and on a tangent to, the exposed membrane where the labelling is most concentrated. Further sections exhibit a ring of intense labelling associated with the apical membrane; this shows a distinct punctate distribution suggestive of subapical cytoplasmic vesicles. No immunoreactivity was evident in the basolateral regions of the cell.

Immunoelectron microscopy

Transmission electron micrographs clearly showed positive H^+-ATPase immunoreactivity localized within cells in the gills of acidotic fish (Figs 6, 7). Immunogold labelling of localized

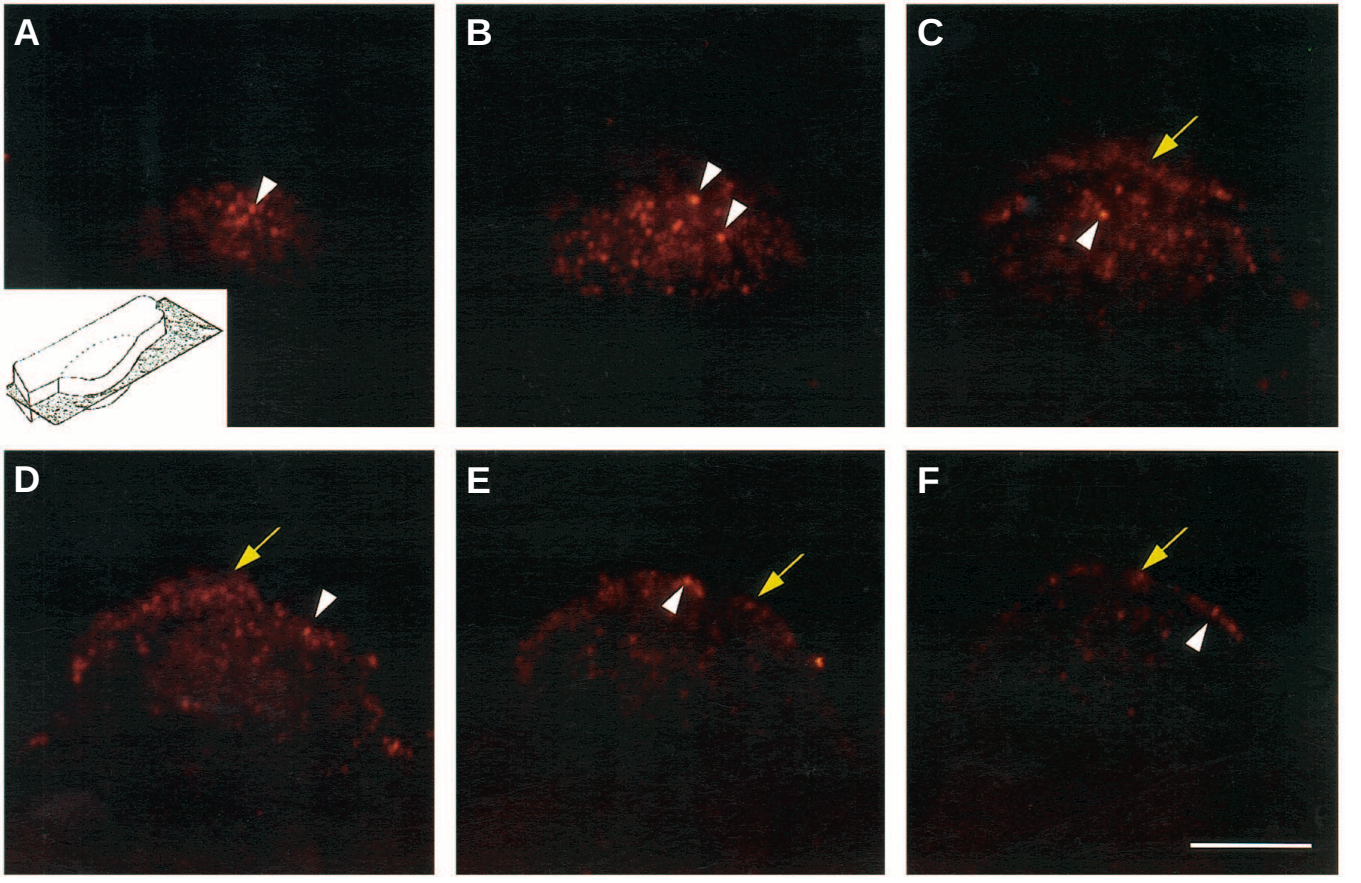

Fig. 5. A series of confocal optical sections made through one cell from the lamella of a fish exposed to 18 h of hypercapnia. Optical sections were made by scanning the section at increasing depths from the apex of the cell to a plane at approximately the middle of the cell. Yellow arrows indicate immunoreactivity associated with the outer apical membrane. White arrowheads indicate immunoreactivity associated with cytoplasmic vesicles. The inset in A represents the orientation of the planes of section. Scale bar, 8 μm.

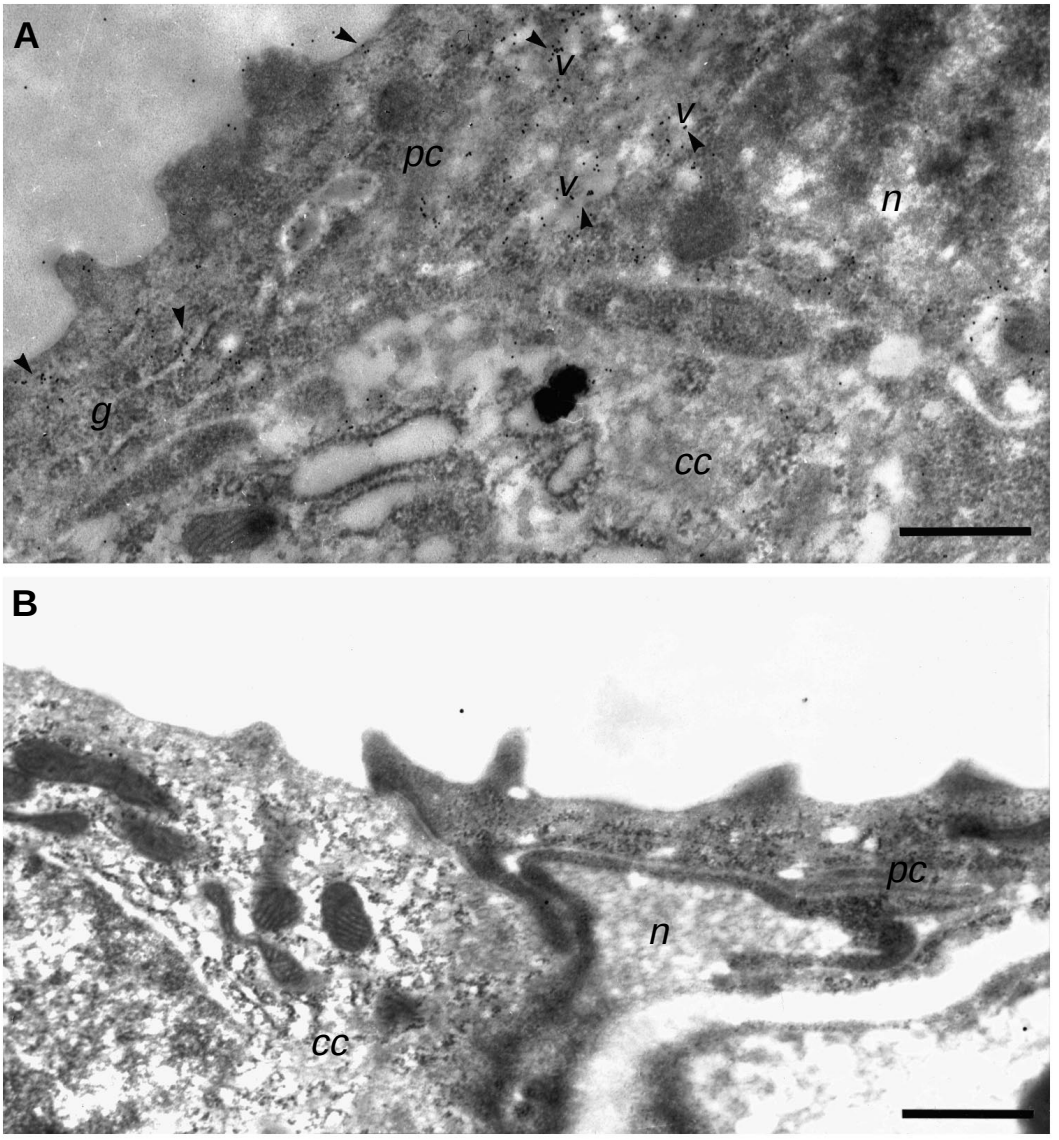

Fig. 6. Transmission electron micrographs of gill sections from fish incubated with proton pump antiserum. (A) A pavement cell (*pc*) and a chloride cell (*cc*) from a fish exposed to 18 h of hypercapnia. Note the positive immunoreactivity (5 nm gold particles depicted by arrowheads) associated with the pavement cell in the vicinity of the apical membrane as well as the Golgi complex (*g*) and cytoplasmic vesicles (*v*). *n*, nucleus. (B) An adjacent chloride cell and pavement cell from a normocapnic fish. Note the absence of any immunoreactivity. Scale bars, 500 nm.

sites was present in pavement cells, particularly associated with the apical membrane and also the apical region of the cytoplasm (Figs 6, 7). The pavement cells of normocapnic fish expressed greatly reduced or no immunogold labelling of H^+-ATPase in any region of the cell (Fig. 6B). It is likely that the total absence of labelling in the gills of normocapnic fish, in part, reflected the extreme thinness of the electron microscope sections (0.1 % of the thickness of the paraffin sections used for light microscopy).

Close examination of the apical region of pavement cells from hypercapnic fish (Figs 6A, 7) not only revealed labelling on the apical membrane, but also distinct concentrations of gold particles in the cytoplasm and in association with the Golgi bodies. Furthermore, there was considerable immunoreactivity in the proximity of vesicles, which appear as electron-lucent 'voids' in the micrographs (Figs 6A, 7). In order to optimize immunolabelling, fixation with osmium tetroxide could not be performed and thus the visualization of cell membranes was impaired. Immunolabelling was essentially abolished when sections were incubated with secondary antibody only, with pre-immune serum or with primary antiserum pre-incubated with excess antigen.

Fig. 6A is a high-magnification transmission electron micrograph showing a pavement cell overlying a chloride cell. In this particular section, positive immunoreactivity was restricted to the pavement cell, with no apparent labelling within the chloride cell. This pattern of immunoreactivity was observed on numerous occasions.

Western blotting

Western blots of gill tissue from hypercapnic and normocapnic fish resulted in pronounced immunoreactive bands at 31 kDa (Fig. 8) when incubated with primary antiserum. The immunoreactive band of the hypercapnic fish appeared to be more intense than that of the normocapnic fish, but both were located at the same molecular mass. Immunoreactive bands were absent on the blots incubated with pre-immune serum in place of antiserum.

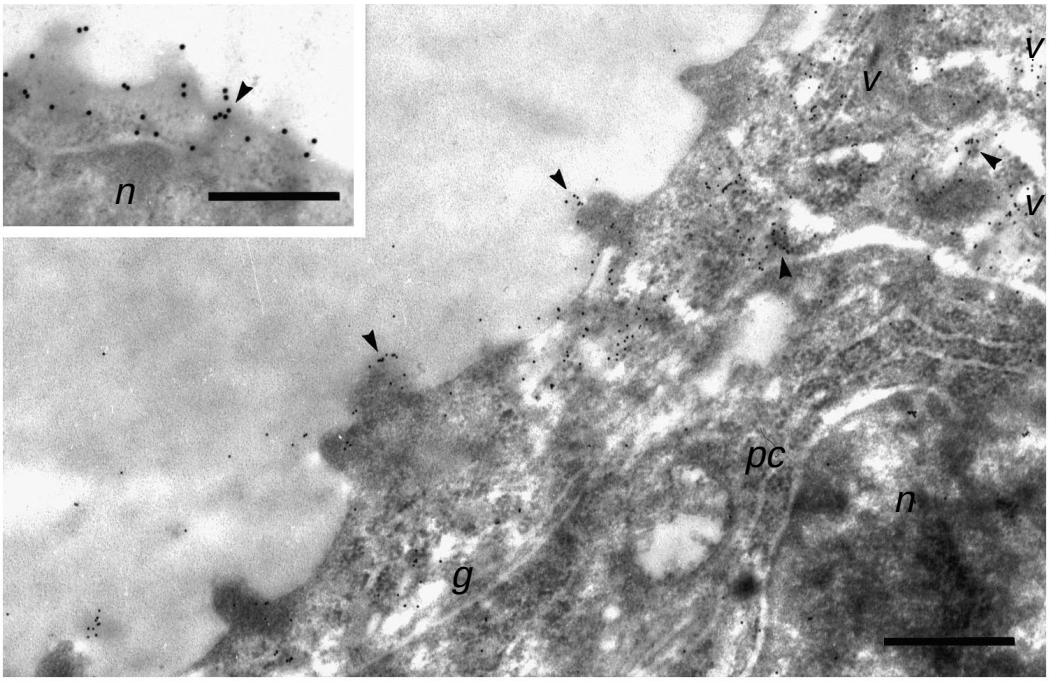

Fig. 7. A pavement cell (*pc*) displaying immunoreactivity (5 nm gold partices depicted by arrowheads) associated with the apical membrane as well as cytoplasmic vesicles (*v*) and Golgi complex (*g*). Vesicles appear to be in the process of migrating from the Golgi complex to the apical membrane. Inset: apical region of a single pavement cell after 18 h of hypercapnia. Note the immunoreactivity associated with the apical membrane and apical regions of the cytoplasm (a 20 nm gold particle is depicted by an arrowhead). *n*, nucleus. Scale bars, 500 nm.

Discussion

This is only the second study to demonstrate proton pump (H^+-ATPase) immunoreactivity in fish gill (see also Lin *et al.* 1994) and it is the first to provide direct evidence that the proton pump is located in lamellar pavement cells. Furthermore, the simultaneous assessment of branchial net acid excretion and proton pump immunoreactivity during hypercapnia employed in the present study has clearly identified 'up-regulation' of the proton pump as an important mechanism of acid–base regulation during respiratory acidosis.

Currently, homologous antibodies to fish gill proton pump subunits are unavailable. Thus, as in the study of Lin *et al.* (1994), non-homologous antibodies were used for immunolocalization. The polyclonal antibody used in the present study was raised in rabbits against a synthetic peptide (CGANANRKFLD), which consists of the carboxy-terminal 11 residues of the predicted 226 amino acid sequence of the 31 kDa subunit of bovine H^+-ATPase (Hirsch *et al.* 1988). Preliminary experiments established that this antibody recognizes the mammalian proton pump antigen based on positive specific immunoreactivity in the intercalated cells of rat kidney (Y. Okawara, personal communication) and thus it was deemed suitable for testing in the fish gill. The specificity in the fish gill was established by comparing labelling patterns in a variety of control situations including pre-absorption of the antibody with excess antigen, application of secondary antibody alone, and the use of pre-immune serum instead of antiserum. In addition, western blotting revealed a single immunoreactive band corresponding to a molecular mass of 31 kDa (Fig. 8). These experiments clearly established the specificity of the antibody and, together with the apical polarization of the labelling and the obvious correlation between the distribution and intensity of immunoreactivity

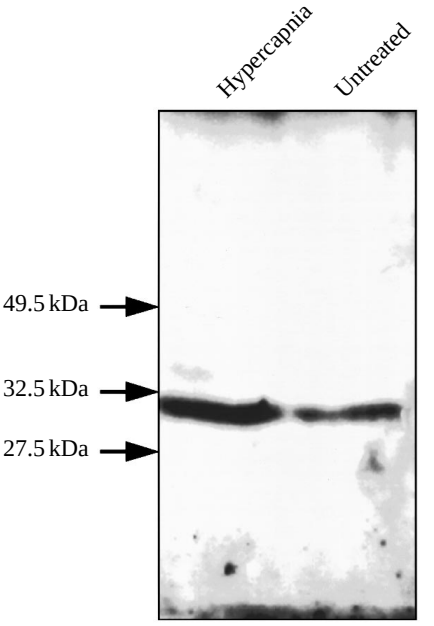

Fig. 8. Representative immunoblot from the gill tissue of rainbow trout demonstrating a single immunoreactive band corresponding to a molecular mass of 31 kDa. Note the increased intensity of the immunoreactive band in the tissue obtained from hypercapnic fish.

with branchial net acid excretion, provide convincing evidence that the antibody is recognizing trout proton pump antigenicity. Finally, the amino acid sequence of the same 31 kDa bovine subunit was used to generate an oligonucleotide mRNA probe that also specifically labelled rat kidney intercalated cells (Fryer *et al.* 1994) and trout lamellar epithelial cells (Sullivan *et al.* 1994). Thus, we agree with Lin *et al.* (1994) that a non-homologous antibody may be used to localize fish H^+-ATPase

when appropriate control experiments have been performed for validation.

The presence of proton pump immunoreactivity in the trout gill supports the alternative model of Na^+ uptake across the gills of freshwater fish (Avella and Bornancin, 1989) which incorporates inward Na^+ movement through apical membrane Na^+ channels. In this scheme, the electrochemical gradient for inward Na^+ movement is, in part, provided by electrogenic outward H^+ pumping. Although the existence of a proton pump in trout gill supports the hypothesis of coupled H^+ pumping and diffusive Na^+ influx, it does not preclude the existence of the electroneutral Na^+/H^+ exchange that has been advocated in the classical model of Na^+ uptake in freshwater fishes (Krogh, 1938). However, given the low concentration of Na^+ in fresh water (e.g. $0.15\,mmol\,l^{-1}$ in City of Ottawa tapwater) and the relatively high concentration of Na^+ in pavement cells (e.g. $60\,mmol\,l^{-1}$ in pavement cells of brown trout *Salmo trutta*; Morgan *et al.* 1994), an electroneutral Na^+/H^+ exchanger seems unlikely. Such a scheme is more likely in the gills of seawater-adapted fishes, in which the concentration of external Na^+ is high (approximately $450\,mmol\,l^{-1}$). Indeed, Lin *et al.* (1994) reported a significant reduction in proton pump immunoreactivity in the gills of seawater-adapted rainbow trout.

On the basis of the Na^+ concentration measured in the pavement cells of brown trout, Morgan *et al.* (1994) estimated that an apical membrane potential of about 130 mV (inside negative) would be required to allow net uptake of Na^+ from dilute fresh water ($0.1\,mmol\,l^{-1}$) through apical membrane Na^+ channels. It is not known whether such large potentials could be generated across the apical membrane. However, the technique utilised by Morgan *et al.* (1994) could not distinguish between free and bound intracellular Na^+, and thus the actual intracellular activities of Na^+ could conceivably have been markedly lower. If so, the required apical membrane potential would also be lowered.

In teleost fish, respiratory acidosis is regulated metabolically by the gradual accumulation of bicarbonate within the extracellular fluid compartments (for reviews, see Cameron, 1978; Randall *et al.* 1982; Heisler, 1984). Such a compensatory mechanism was clearly evident in the present study. The accumulation of bicarbonate is predominantly achieved by an increase in branchial acid excretion and, to a lesser extent, by increased renal acid excretion (e.g. Perry *et al.* 1987*a*,*b*). Previous research has identified two mechanisms that contribute to the increased branchial acid excretion during respiratory acidosis, a reduced rate of Cl^-/HCO_3^- exchange and an accelerated rate of Na^+/H^+ exchange (for reviews, see Cameron, 1989; Cameron and Iwama, 1989; McDonald *et al.* 1989; Wood and Goss, 1990; Goss *et al.* 1992*a*). Recently, a series of studies employing morphological techniques have provided evidence that the mechanism of reduced Cl^-/HCO_3^- exchange during respiratory acidosis is a physical covering of chloride cells by neighbouring pavement cells (Goss *et al.* 1992*a*, 1994*a*,*b*; Goss and Perry, 1993). This is believed to uncouple Cl^-/HCO_3^- exchange sites (on chloride cell apical membranes) from the water and thus to constrain Cl^-/HCO_3^- exchange (see reviews by Goss *et al.* 1992*a*; Perry and Laurent, 1993). Conversely, during alkalosis, the surface area of exposed chloride cells increases, and this is thought to contribute to the compensatory increase in Cl^-/HCO_3^- exchange that is observed at such times (Goss and Perry, 1994; Perry and Goss, 1994).

In the light of the recent empirical evidence and theoretical considerations (see above), stimulation of Na^+/H^+ exchange is unlikely to contribute significantly, if at all, to enhanced branchial acid excretion during acidosis. Nevertheless, the obvious correlation between proton pump immunoreactivity and net acid excretion observed in this study suggests that electrogenic proton pumping is an important mechanism of branchial net acid excretion. Thus, the increase in Na^+ uptake that often accompanies respiratory acidosis may reflect indirect coupling *via* the proton pump/Na^+ channel mechanism rather than direct coupling *via* Na^+/H^+ exchange (see also Potts, 1994).

The distinct apical polarization of proton pump immunoreactivity in trout gill and its apparent localization in subapical cytoplasmic vesicles is reminiscent of the situation in other acid-secreting epithelia in which vesicles containing proton pumps fuse with the apical plasma membrane during acidosis to form active domains of intense proton pump activity (Gluck *et al.* 1982*b*; Brown *et al.* 1988, 1992; Gluck and Nelson, 1992). In addition to the possible cellular redistribution of proton pumps, the increased immunoreactivity during hypercapnic acidosis was, at least in part, a result of increased proton pump synthesis as revealed by the western blots. We have recently shown, using *in situ* hybridization, an increase in the expression of the mRNA for the 31 kDa subunit of the proton pump in hypercapnic trout (G. Sullivan, J. Fryer and S. Perry, unpublished results), which lends support to the hypothesis of increased proton pump synthesis during respiratory acidosis.

The presence of a proton pump in the trout gill pavement cell is in stark contrast to other acid-excreting epithelia such as frog skin (Ehrenfeld *et al.* 1985), turtle urinary bladder (Gluck *et al.* 1982*a*) and mammalian renal collecting duct (Brown *et al.* 1992). In those epithelia, the proton pump is located exclusively in mitochondria-rich cells that are structurally analogous to the fish gill chloride cell. However, the finding of proton pump immunoreactivity in the trout pavement cell was expected given the results of several previous indirect studies. In particular, Goss *et al.* (1992*b*, 1994*a*) observed that the gill pavement cells of brown bullhead (*Ictalurus nebulosus*) undergo a pronounced morphological transformation during hypercapnic acidosis when the numbers of mitochondria and the surface area of apical membrane microvilli increase markedly. These changes occur concomitantly with increased branchial acid excretion and Na^+ uptake. More recently, Laurent *et al.* (1994) reported the occurrence of vesicles in brown bullhead pavement cells that were similar in structure to the proton pump vesicles reported in other acid-secreting epithelia (e.g. Brown *et al.* 1987).

Moreover, the numbers of cytoplasmic vesicles and the occurrence of pear-shaped pits (indicative of vesicle fusion with the plasma membrane) were increased during hypercapnia (Laurent *et al.* 1994). Proton pump vesicles and pear-shaped pits were not observed in chloride cells. Thus, the increased surface area of pavement cell apical membrane microvilli during hypercapnia noted by Goss *et al.* (1992*b*) may represent insertion of proton pump vesicles into the apical plasma membrane, while the increased numbers of mitochondria presumably correspond to the increased energetic requirements of pavement cell proton pump activity. Acid excretion by proton pump activity requires the presence of carbonic anhydrase and, indeed, the fish gill pavement cell is known to contain abundant carbonic anhydrase activity (Rahim *et al.* 1988). Clearly, in the light of the current study and other recent evidence (Goss *et al.* 1992*b*; Laurent *et al.* 1994), the traditional view that the fish gill pavement cell is involved only in respiratory gas transfer is probably incorrect. Indeed, Potts (1994), in a recent editorial review, hypothesized that Na^+ uptake is confined to the pavement cells while Cl^- uptake occurs in the chloride (mitochondria-rich) cells.

Although the results of this study demonstrate proton pump immunoreactivity in pavement cells, we cannot totally exclude its presence in chloride cells because insufficient numbers of chloride cells were examined. The focus of this study was the pavement cell, and there was no attempt to quantify the distribution of proton pump immunoreactivity in the various cell types of the gill. However, the results of several other studies indicate that the chloride cell may not contain proton pump activity. First, during hypercapnic acidosis in brown bullhead (Goss *et al.* 1992*b*) and rainbow trout (Goss and Perry, 1993), gill chloride cells are covered by pavement cells during periods of intense branchial acid excretion. Second, Laurent *et al.* (1994) failed to observe proton pump vesicles in chloride cells during an extensive analysis of brown bullhead gills. Clearly, further work will be required to clarify the roles of the pavement cell and chloride cell in acid–base regulation in freshwater fishes.

We thank Dr Yuji Okawara and F. Ayoub for assistance with immunocytochemistry, V. Kapal for assistance with electron microscopy and A. Vailant for technical assistance with confocal microscopy and immunoblotting. This research was supported by a grant from the Natural Sciences and Engineering Research Council (NSERC) of Canada awarded to S.F.P. and a grant from the Medical Research Council (MRC) of Canada awarded to J.N.F.

References

AVELLA, M. AND BORNANCIN, M. (1989). A new analysis of ammonia and sodium transport through the gills of the freshwater rainbow trout (*Salmo gairdneri*). *J. exp. Biol.* **142**, 155–175.

AVELLA, M. AND BORNANCIN, M. (1990). Ion fluxes in the gills of freshwater and seawater salmonid fish. In *Animal Nutrition and Transport Processes.* 2. *Transport, Respiration and Excretion: Comparative and Environmental Aspects* (ed. J. P. Truchot and B. Lahlou). Basel: Karger. *Comparative Physiology*, vol. 6, pp. 119–136.

BOUTILIER, R. G., HEMING, T. A. AND IWAMA, G. K. (1984). Physiochemical parameters for use in fish respiratory physiology. In *Fish Physiology*, vol. XA (ed. W. S. Hoar and D. J. Randall), pp. 403–430. New York: Academic Press.

BROWN, D., GLUCK, S. AND HARTWIG, J. (1987). Structure of the novel membrane-coating material in proton-secreting epithelial cells and identification as an H^+ATPase. *J. Cell Biol.* **105**, 1637–1648.

BROWN, D., HIRSCH, S. AND GLUCK, S. (1988). Localization of a proton-pumping ATPase in rat kidney. *J. clin. Invest.* **82**, 2114–2126.

BROWN, D., SABOLIC, I. AND GLUCK, S. (1992). Polarized targeting of V-ATPase in kidney epithelial cells. *J. exp. Biol.* **172**, 231–243.

CAMERON, J. N. (1978). Regulation of blood pH in teleost fish. *Respir. Physiol.* **33**, 129–144.

CAMERON, J. N. (1989). Acid–base homeostasis: past and present persepctives. *Physiol. Zool.* **62**, 845–865.

CAMERON, J. N. AND IWAMA, G. K. (1989). Compromises between ionic regulation and acid–base regulation in aquatic animals. *Can. J. Zool.* **67**, 3078–3084.

EHRENFELD, J., GARCIA-ROMEU, F. AND HARVEY, B. J. (1985). Electrogenic active proton pump in *Rana esculenta* skin and its role in sodium ion transport. *J. Physiol., Lond.* **359**, 331–355.

EVANS, D. H. (1993). Osmotic and ionic regulation. In *The Physiology of Fishes* (ed. D. H. Evans), pp. 315–341. Boca Raton: CRC Press.

FRYER, J. N., OKAWARA, Y., WELD, M. AND LEVINE, D. Z. (1994). Modulation of A-type intercalated cell H^+-ATPase gene expression by metabolic acidosis and metabolic alkalosis. *CFBS 37th Annual Meeting, Conference Proceedings*. Abstr no. **543**, p157.

GLUCK, S., CANNON, C. AND AL-AWQATI, Q. (1982*a*). Exocytosis regulates urinary acidification in turtle bladder by rapid insertion of H^+ pumps into the luminal membrane. *Proc. natn. Acad. Sci. U.S.A.* **79**, 4327–4331.

GLUCK, S., KELLY, S. AND AL-AWQATI, Q. (1982*b*). The proton translocating ATPase responsible for urinary acidification. *J. biol. Chem.* **267**, 9230–9233.

GLUCK, S. AND NELSON, R. (1992). The role of the V-ATPase in renal epithelial H^+ transport. *J. exp. Biol.* **172**, 205–218.

GOSS, G. G., LAURENT, P. AND PERRY, S. F. (1992*a*). Evidence for a morphological component in the regulation of acid–base balance in hypercapnic catfish (*Ictalurus nebulosus*). *Cell. Tissue Res.* **268**, 539–552.

GOSS, G. G., LAURENT, P. AND PERRY, S. F. (1994*a*). Gill morphology during hypercapnia in brown bullhead (*I. nebulosus*): Role of chloride cells and pavement cells in acid–base regulation. *J. Fish Biol.* **45**, 705–718.

GOSS, G. G., LAURENT, P. AND PERRY, S. F. (1995). Gill morphology and acid–base regulation. In *Fish Physiology*, vol. 14 (ed. W. S. Hoar, D. J. Randall and A. P. Farell), pp. 257–284. New York: Academic Press.

GOSS, G. G. AND PERRY, S. F. (1993). Physiological and morphological regulation of acid–base status during hypercapnia in rainbow trout (*Oncorhynchus mykiss*). *Can. J. Zool.* **71**, 1673–1680.

GOSS, G. G. AND PERRY, S. F. (1994). Different mechanisms of acid–base regulation in rainbow trout (*Oncorhynchus mykiss*) and American eel (*Anguilla rostrata*) during $NaHCO_3$ infusion. *Physiol. Zool.* **67**, 381–406.

GOSS, G. G., PERRY, S. F., WOOD, C. M. AND LAURENT, P. (1992*b*).

Mechanisms of ion and acid–base regulation at the gills of freshwater fish. *J. exp. Zool.* **263**, 143–159.

GOSS, G. G., WOOD, C. M., LAURENT, P. AND PERRY, S. F. (1994*b*). Morphological responses of the rainbow trout (*Oncorhynchus mykiss*) gill to hyperoxia, base ($NaHCO_3$) and acid (HCl) infusions. *Fish Physiol. Biochem.* **12**, 465–477.

HEISLER, N. (1984). Acid–base regulation in fishes. In *Fish Physiology*, vol. XA (ed. W. S. Hoar and D. J. Randall), pp. 315–401. New York: Academic Press.

HIRSCH, S., STRAUSS, A., MASOOD, K., LEE, S., SUKHATME, V. AND GLUCK, S. (1988). Isolation and sequence of a cDNA encoding the 31-kDa subunit of bovine kidney vacuolar H^+-ATPase. *Proc. natn. Acad. Sci. U.S.A.* **85**, 3004–3008.

KROGH, A. (1938). The active absorption of ions in some freshwater animals. *Z. vergl. Physiol.* **25**, 335–350.

LAEMMLI, U. K. (1970). Cleavage of structural proteins during the assembly of the head of bateriophage T4. *Nature* **27**, 580–585.

LAURENT, P., GOSS, G. G. AND PERRY, S. F. (1994). Proton pumps in fish gill pavement cells. *Archs. int. Physiol. Biochim. Biophys.* **102**, 77–79.

LIN, H., PFEIFFER, D. C., VOGL, A. W., PAN, J. AND RANDALL, D. J. (1994). Immunolocalization of H^+-ATPase in the gill epithelia of rainbow trout. *J. exp. Biol.* **195**, 169–183.

LIN, H. AND RANDALL, D. J. (1991). Evidence for the presence of an electrogenic proton pump on the trout gill epithelium. *J. exp. Biol.* **161**, 119–134.

LIN, H. AND RANDALL, D. J. (1993). Proton-ATPase activity in the crude homogenates of fish gill tissue: inhibitor sensitivity and environmental and hormonal regulation. *J. exp. Biol.* **180**, 163–174.

MCDONALD, D. G., TANG, Y. AND BOUTILIER, R. G. (1989). Acid and ion transfer across the gills of fish: mechanisms and regulation. *Can. J. Zool.* **67**, 3046–3054.

MCDONALD, D. G. AND WOOD, C. M. (1981). Branchial and renal acid and ion fluxes in the rainbow trout, *Salmo gairdneri*, at low environmental pH. *J. exp. Biol.* **93**, 101–118.

MORGAN, I. J., POTTS, W. T. W. AND OATES, K. (1994). Intracellular ion concentrations in branchial epithelial cells of brown trout (*Salmo trutta* L.) determined by X-ray microanalysis. *J. exp. Biol.* **194**, 139–151.

PERRY, S. F. AND GOSS, G. G. (1994). The effects of experimentally altered gill chloride cell surface area on acid–base regulation in rainbow trout during metabolic alkalosis. *J. comp. Physiol.* A **164**, 327–336.

PERRY, S. F. AND LAURENT, P. (1993). Environmental effects on fish gill structure and function. In *Fish Ecophysiology* (ed. J. C. Rankin and F. B. Jensen), pp. 231–264. London: Chapman & Hall.

PERRY, S. F., MALONE, S. AND EWING, D. (1987*a*). Hypercapnic acidosis in the rainbow trout (*Salmo gairdneri*). I. Branchial ionic fluxes and blood acid–base status. *Can. J. Zool.* **65**, 888–895.

PERRY, S. F., MALONE, S. AND EWING, D. (1987*b*). Hypercapnic acidosis in rainbow trout (*Salmo gairdneri*). II. Renal ionic fluxes. *Can. J. Zool.* **65**, 896–902.

POTTS, W. T. W. (1994). Kinetics of sodium uptake in freshwater animals – a comparison of ion-exchange and proton pump hypotheses. *Am. J. Physiol.* **266**, R315–R320.

RAHIM, S. M., DELAUNOY, J. P. AND LAURENT, P. (1988). Identification and immunocytochemical localization of two different carbonic anhydrase isozymes in teleostean fish erythrocytes and gill epithelia. *Histochemistry* **89**, 451–459.

RANDALL, D. J., PERRY, S. F. AND HEMING, T. A. (1982). Gas transfer and acid–base regulation in salmonids. *Comp. Biochem. Physiol.* B **73**, 93–103.

SHUTTLEWORTH, T. J. (1989). Overview of epithelial ion transport mechanisms. *Can. J. Zool.* **67**, 3032–3038.

SOIVIO, A., NYHOLM, K. AND WESTMAN, K. (1975). A technique for repeated blood sampling of the blood of individual resting fish. *J. exp. Biol.* **62**, 207–217.

SULLIVAN, G. V., PERRY, S. F. AND FRYER, J. N. (1994). Proton pump expression and acid–base status in gill epithelium of rainbow trout, *Oncorhynchus mykiss*. *CFBS 37th Annual Meeting, Conference Proceedings*. Abstr no. **542**, p. 157.

VERDOUW, H., VAN ECHTED, C. J. A. AND DEKKERS, E. M. J. (1978). Ammonia determination based on indophenol formation with sodium salicylate. *Water Res.* **12**, 399–402.

WOOD, C. M. AND GOSS, G. G. (1990). Kinetic analysis of the relationship between ion exchange and acid–base regulation at the gills of freshwater fish. *Animal Nutrition and Transport Processes* **26**, 119–136.